UC Berkeley
UC Berkeley Previously Published Works

Title

Enantioselective Synthesis of N,S-Acetals by an Oxidative Pummerer-Type Transformation using Phase-Transfer Catalysis.

Permalink

Journal

ISSN

Authors

Biswas, Souvagya
Kubota, Koji
Orlandi, Manuel
et al.

Publication Date

DOI

Enantioselective Synthesis of *N,S*-Acetals by an Oxidative Pummerer-Type Transformation using Phase-Transfer Catalysis

Souvagya Biswas[+], Koji Kubota[+], Manuel Orlandi, Mathias Turberg, Dillon H. Miles, Matthew S. Sigman,* and F. Dean Toste*

Abstract: *Reported is the first enantioselective oxidative Pummerer-type transformation using phase-transfer catalysis to deliver enantioenriched sulfur-bearing heterocycles. This reaction includes the direct oxidation of sulfides to a thionium intermediate, followed by an asymmetric intramolecular nucleophilic addition to form chiral cyclic N,S-acetals with moderate to high enantioselectivites. Deuterium-labelling experiments were performed to identify the stereodiscrimination step of this process. Further analysis of the reaction transition states, by means of multidimensional correlations and DFT calculations, highlight the existence of a set of weak noncovalent interactions between the catalyst and substrate that govern the enantioselectivity of the reaction.*

Since its discovery in 1909, the Pummerer reaction and related thionium chemistry have been successfully applied to the synthesis of a variety of synthetically and biologically useful compounds and natural products.[1,2] Mechanistically, Pummerer-type reactions are proposed to proceed by nucleophilic addition to an in situ generated thionium species to form sulfur-containing motifs (Scheme 1a). Despite significant investigation of this transformation, there have been no reports to date describing catalytic enantioselective variants.[3] Development of this transformation would provide an enantioselective entry to carbon stereocenters, bearing sulfur, which were previously deemed either challenging or inaccessible.[4,5]

Given our recent success in applying chiral-anion phase-transfer (CAPT) catalysis to various challenges in asymmetric catalysis (Scheme 1b),[6,7] we envisioned that this strategy may be applied to the enantioselective construction of stereogenic C–S bonds through a Pummerer-type reaction (Scheme 1c). In this scenario, a chiral phosphoric acid (**1**) would generate a chiral phosphate anion (**2**) under basic conditions, and could undergo a salt metathesis with an appropriately identified insoluble cationic oxidant to form
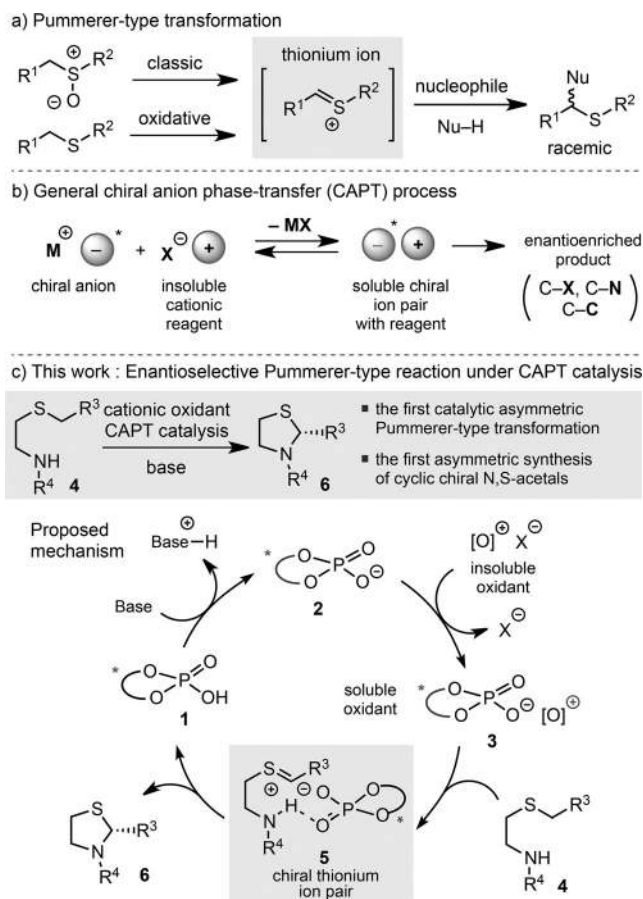
Scheme 1. Application of CAPT catalysis to the oxidative Pummerer-type C–N bond-forming reaction for the synthesis of enantioenriched *N,S*-acetals.

a soluble ion pair (**3**) in a nonpolar solvent. This species (**3**) would then presumably react with the sulfide **4** to generate a chiral thionium ion pair (**5**)[8] which undergoes a nucleophilic attack to provide the enantioenriched product, the cyclic *N,S*-acetal **6**, and release the chiral phosphate. This strategy would enable the first enantioselective construction of cyclic *N,S*-acetal skeletons.[9]

To initiate this study, we first tested Bobbitt's salt **7a** (for structure see Table 1),[10,11] as this reagent was successfully applied to produce an iminium ion pair using CAPT catalysis in an enantioselective cross-dehydrogenative coupling.[7] It should be noted that direct oxidation of sulfides to thionium species using this class of oxidant has not been reported to date.[12] Encouragingly, the reaction of **4a** in the presence of 10 mol% of the (*R*)-TRIP (**1a**) catalyst, the oxidant **7a** (3.0 equiv), and Na₃PO₄ (3.0 equiv) in toluene under air at

[*] Dr. S. Biswas,[+] Dr. K. Kubota,[+] M. Turberg, Dr. D. H. Miles,
Prof. Dr. F. D. Toste
Department of Chemistry, University of California
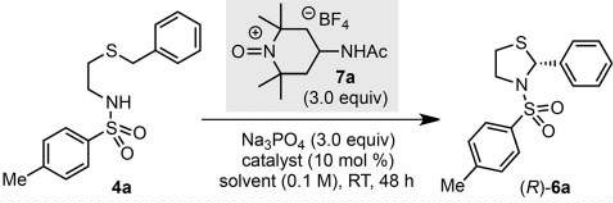Berkeley, CA 94720 (USA)
E-mail: fdtoste@berkeley.edu

Dr. M. Orlandi, Prof. Dr. M. S. Sigman
Department of Chemistry, University of Utah
Salt Lake City, UT 84112 (USA)
E-mail: sigman@chem.utah.edu

[+] These authors contributed equally to this work.

⊟ Supporting information and the ORCID identification number(s) for
the author(s) of this article can be found under:
https://doi.org/10.1002/anie.201711277.

room temperature gave the desired cyclic *N,S*-acetal **6a** in good yield and with promising enantioselectivity (Table 1, entry 1).[13] Introducing alkyl chains onto the binaphthyl backbone of the phosphoric acid (**1b**) to enhance catalyst

Table 1: Optimization of reaction conditions for the enantioselective oxidative Pummerer-type cyclization.[a]

Entry	Catalyst	Solvent	Yield [%][b]	ee [%][c]
1	**1a**	toluene	62	62
2	**1b**	toluene	60	64
3	**1c**	toluene	64	52
4	**1d**	toluene	61	49
5	**1e**	toluene	62	26
6	**1f**	toluene	59	56
7	**1g**	toluene	58	60
8	**1h**	toluene	56	68
9	**1i**	toluene	50	62
10	**1j**	toluene	44	62
11[d]	**1h**	toluene	<5	–
12[e]	**1h**	toluene	22	77
13	**1h**	toluene/EC	60	68
14[f]	**1h**	toluene/EC	55	76

[a] See the Supporting Information for complete optimization data.
[b] Yield of product isolated after silica gel column chromatography.
[c] Determined by HPLC analysis using a chiral stationary phase.
[d] Reaction was carried out with nitrosyl tetrafluoroborate salt (**7b**) as the oxidant and gave complex mixture of products. [e] Reaction was carried out with 2,2,6,6-tetramethylpiperidine-1-oxoammonium tetra-fluroborate salt (**7c**) as oxidant. [f] Reaction was carried out at 0°C. EC = ethylcyclohexane.

solubility marginally improved the enantioselectivity of the reaction (entry 2). Unfortunately, the use of another conventional phosphoric acid (TCYP; **1c**; entry 3) resulted in lower enantioselectivity. To probe steric effects, various other phosphates displaying unique substitution patterns were examined. This systematic investigation (entries 4–10) revealed that the substituent R^2, on the 3,3′-phenyl ring, is crucial (entry 6) and that a bulky R^3 substituent further improved the enantioselectivity (entries 8–10). To further explore improvements to the reaction, a stronger cationic oxidant, nitrosyl tetrafluoroborate salt (**7b**), was evaluated but unfortunately gave a complex mixture of products (entry 11). Interestingly, the structurally analogous oxidant, 2,2,6,6-tetramethylpiperidine-1-oxoammonium tetrafluoro-

borate salt (**7c**), improved the enantioselectivity significantly, although a poor yield was observed (entry 12).[14] Finally, we found that the use of toluene/ethylcyclohexane (EC) as a cosolvent system at 0°C resulted in formation of the product in improved enantioselectivity (entry 14).

By using this set of reaction conditions, the scope of this process was explored as depicted in Table 2. Aryl sulfonamides bearing both electron-rich and electron-poor groups at the *para* position were tolerated, thus resulting in moderate to good enantioselectivities (**6a–d**). While methyl substituents on the sulfonamide backbone (**6a–d**) did not improve the enantioselectivities (**6e,f**), the 1-naphthyl substrate **4g** afforded the product (*R*)-**6g** in high enantiomeric excess. We next turned our attention to the scope with respect to the benzyl sulfide moiety using the 1-naphthyl sulfonamide backbone (Table 2b). Benzylic groups bearing both electron-rich (**6i–k**, **6u**) and electron-poor groups (**6l–o**, **6r–t**) were tolerated to furnish the corresponding *N,S*-acetal products with good to high enantioselectivities. Notably, substrates having a sterically hindered substituent (**6j**) and *meta* substituents (**6p**, **6r–t**) were prone to giving higher *ee* values. Moreover, the developed reaction conditions were readily applicable to the enantioselective synthesis of six-membered *N,S*-acetals (**8a–e**, Table 2c) and substrates bearing different N nucleophiles (**9** and **10**, Table 2d). Unfortunately, substrates bearing an electron-deficient 4-nitrobenzyl group were not oxidized under the reaction conditions (Table 2e).

A series of experiments were conducted to gain insight into the reaction mechanism. Reaction of the sulfoxide **11** under both the optimized phase-transfer and non-enantioselective conditions resulted in no observed product, thus discounting a sulfoxide-mediated mechanism (Scheme 2a). These results are consistent with the proposed phase-transfer mechanism, which includes direct oxidation of a sulfide to a thionium cation using an oxoammoium-phosphate chiral ion pair (Scheme 1c). We sought to establish whether the enantioselectivity was determined during substrate oxidation or the cyclization of the oxidized intermediate. Although the stereogenic center of the product **6** (Scheme 1c) is formally set in the cyclization of the oxidized intermediate (**5**), substrate–catalyst interactions during the oxidation event may preorganize the system for the enantioselective cycliza-
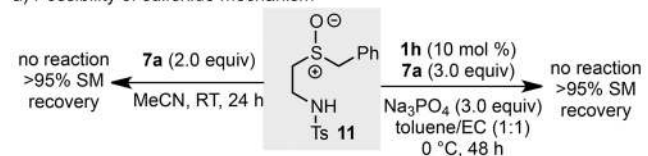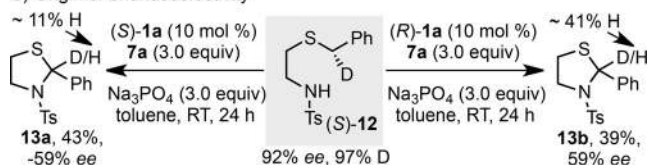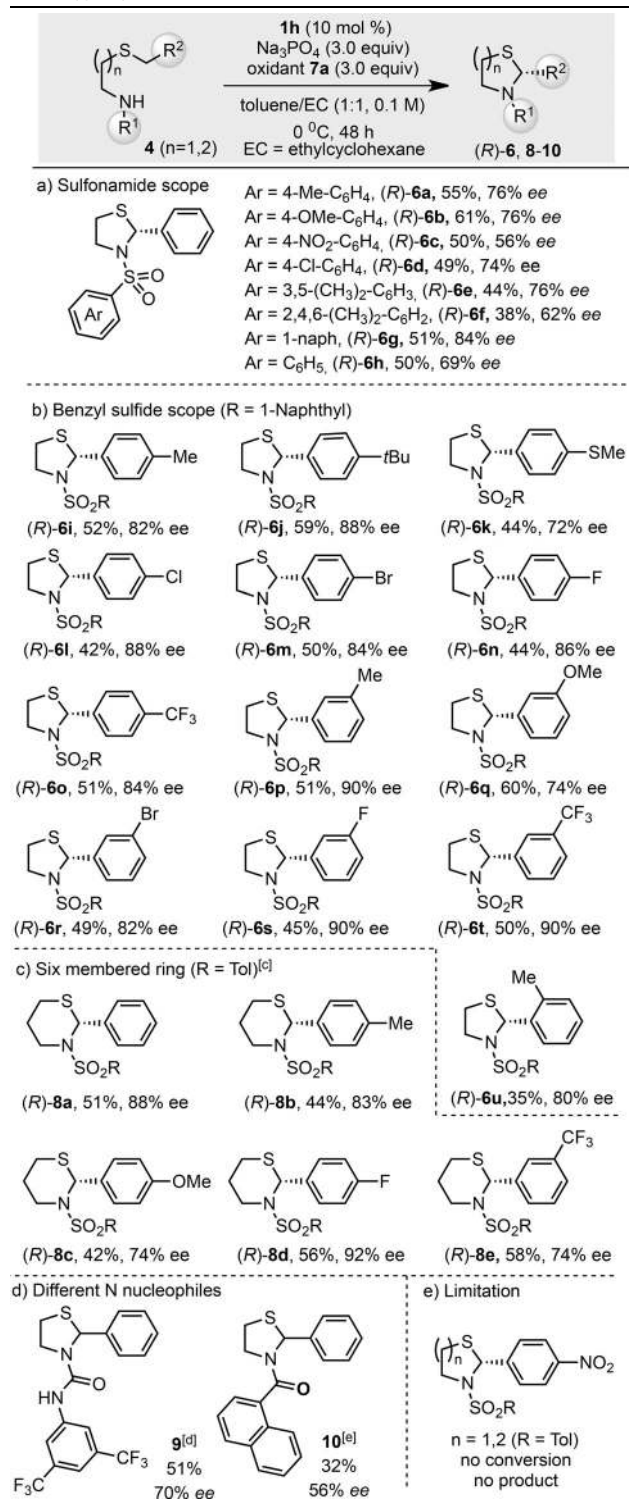

Scheme 2. Mechanistic investigations.

Table 2: Scope and limitations of the enantioselective oxidative Pummerer-type cyclization.[a,b]

a) Sulfonamide scope

Ar = 4-Me-C₆H₄, (R)-**6a**, 55%, 76% *ee*
Ar = 4-OMe-C₆H₄, (R)-**6b**, 61%, 76% *ee*
Ar = 4-NO₂-C₆H₄, (R)-**6c**, 50%, 56% *ee*
Ar = 4-Cl-C₆H₄, (R)-**6d**, 49%, 74% ee
Ar = 3,5-(CH₃)₂-C₆H₃, (R)-**6e**, 44%, 76% *ee*
Ar = 2,4,6-(CH₃)₂-C₆H₂, (R)-**6f**, 38%, 62% *ee*
Ar = 1-naph, (R)-**6g**, 51%, 84% *ee*
Ar = C₆H₅, (R)-**6h**, 50%, 69% *ee*

b) Benzyl sulfide scope (R = 1-Naphthyl)

(R)-**6i**, 52%, 82% ee
(R)-**6j**, 59%, 88% ee
(R)-**6k**, 44%, 72% ee
(R)-**6l**, 42%, 88% ee
(R)-**6m**, 50%, 84% ee
(R)-**6n**, 44%, 86% ee
(R)-**6o**, 51%, 84% ee
(R)-**6p**, 51%, 90% ee
(R)-**6q**, 60%, 74% ee
(R)-**6r**, 49%, 82% ee
(R)-**6s**, 45%, 90% ee
(R)-**6t**, 50%, 90% ee

c) Six membered ring (R = Tol)[c]

(R)-**8a**, 51%, 88% ee
(R)-**8b**, 44%, 83% ee
(R)-**6u**, 35%, 80% ee
(R)-**8c**, 42%, 74% ee
(R)-**8d**, 56%, 92% ee
(R)-**8e**, 58%, 74% ee

d) Different N nucleophiles

9[d]
51%
70% ee

10[e]
32%
56% ee

e) Limitation

n = 1,2 (R = Tol)
no conversion
no product

[a] Yields of isolated products are shown. Remainder of the mass balance is starting material and products derived from oxidative debenzylation of the sulfide. [b] The *ee* values were determined by HPLC analysis using a chiral stationary phase. The absolute configuration of **6a** was established by the comparison of the retention time from the HPLC analysis of the authentic optically active sample. The structures of other products were assigned by analogy. [c] **1c** was used as a catalyst. [d] H₈-TCYP was used as a catalyst at −30°C. [e] **1b** was used as a catalyst.

tion. To examine these possibilities, the enantiopure substrate (*S*)-**12** (92% *ee*, 97% D incorporation) was subjected to the oxidative Pummerer-type cyclization (Scheme 2b). The observation that the isolated products (**13a** and **13b**) exhibited equal but opposite levels of enantioselectivity, with different levels of H incorporation, is consistent with a mechanism in which the chiral phosphate is involved in substrate oxidation, but the redox event is decoupled from the enantiodetermining cyclization.

Multidimensional correlation analysis was performed to gain additional information about the features of the catalyst that contribute to the stereoselectivity.[15] A set of parameters for several phosphates (**1a–h**; see the Supporting Information for a full set of catalysts) was computed using the molecular model in Figure 1a.[16] This parameter set included IR vibrational frequencies (ν),[17] and intensities (i),[17] NBO charges, and Sterimol steric descriptors (*B1*, *B5* and *L*).[18] When the acquired parameters were correlated with the measured *ee* values, expressed as $\Delta\Delta G^{\ddagger}$, the multidimensional model in Figure 1a was obtained. This model presented a good correlation ($R^2 = 0.96$, intercept = 0.03) and was statistically validated by the leave-one-out cross validation (L1O = 0.89). Three Sterimol parameters appeared in the equation: *B5*, maximum width of the entire catalysts' aryl substituent; *B1₂* and *B1₄*, minimum width of the substituents in the 2,6-positions and of the substituent in the 4-position of the aryl group, respectively. *B1₂* presented the largest coefficient and accounted for the necessity of large groups in the 2,6-positions. However, despite enhancements provided by bulky 2,6-groups, increasing their length negatively impacts the *ee* value as highlighted by the presence of the parameter *B5*, with a negative coefficient. Finally, the smallest coefficient was associated with *B1₄*, which accounted for fine tuning resulting from the presence of substituents with increasing size at the 4-position of the phosphate aryl group (compare catalysts **1a** with **1g–j**).[19]

Further information about the interaction mode between the catalyst and the substrate was gained by transition-state (TS) analysis of the reaction between **1a** and **4h**. As the deuterium-labelling experiments suggested that the thionium ring closure is stereodetermining, computations were focused on this reaction step. The low-lying TSs leading to the *R*- and *S*-configured products (**TS-R** and **TS-S**, respectively) are depicted in Figure 1c (see the Supporting Information for computational details). **TS-R** is favored and consistent with the experimentally observed product configuration, and the relative energy of **TS-S** (1.03 kcal mol⁻¹) matched with the selectivity measured experimentally (56% *ee*, 0.75 kcal mol⁻¹). The two TSs showed several NCIs between the phosphate and the substrate.[20] However, **TS-R** displayed a better accommodation of the benzenesulfonamide group through CH–π interactions, which involved the *i*Pr substituents and the binaphthyl backbone of the catalyst.[17b,21] This representation provides an interpretation for the statistical model in Figure 1a. Additionally, a stronger CH–π interaction between the aryl substituent (*i*Pr₃Ph) of the catalyst and the electron-deficient alkyl chain of the substrate was present in **TS-R** (three CH–π contacts, while **TS-S** presents only one CH–π contact).
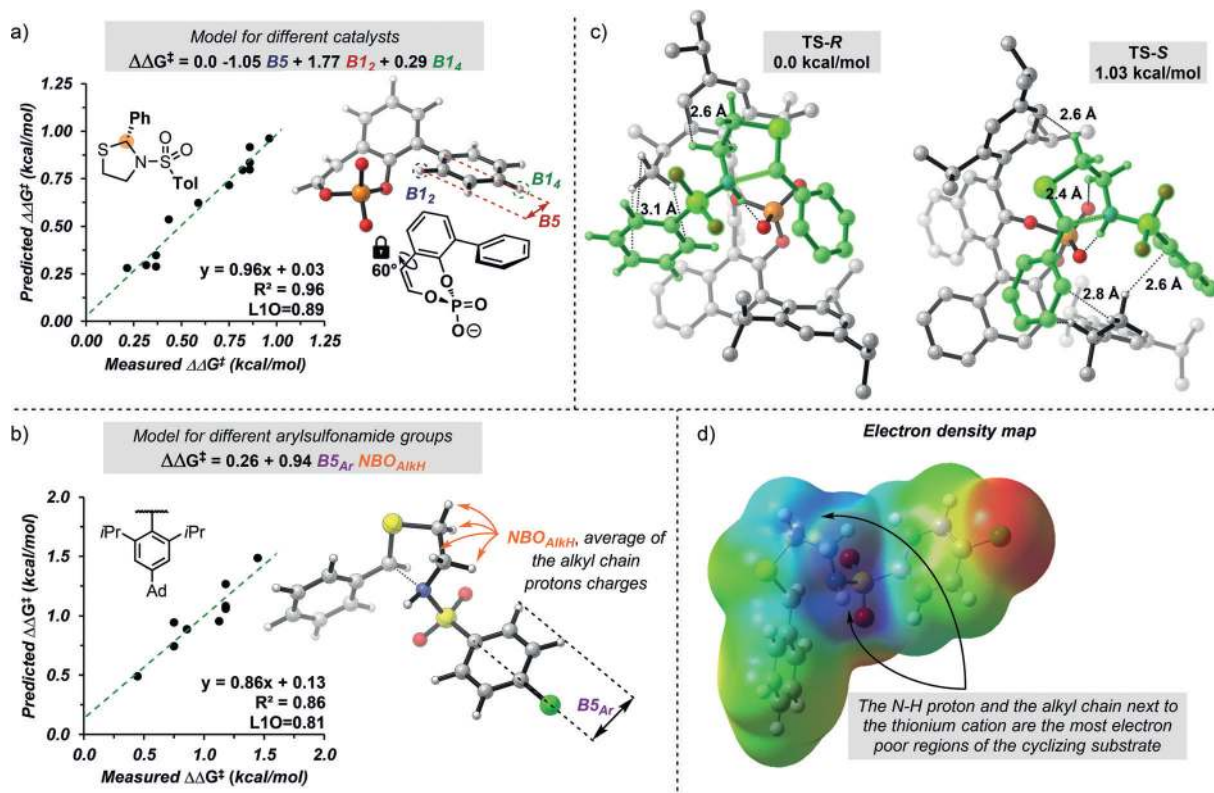
Figure 1. Multidimensional correlation analysis for the catalysts **1a–h** (a) and the substrates **4a–4h** (b). c) **TS-R** and **TS-S** computed at the wB97XD/6-31G(d) level of theory. wB97XD/6–311＋G(2d,p)[PCM＝Tol] energies are reported. The substrate is highlighted in green and interatomic distances are shown as dashed lines. d) Electron density map of the uncatalyzed **TS** of **6d**.

The importance of this interaction in the stereochemical recognition was also highlighted by multidimensional analysis of the arylsulfonylamide group of the substrate. Descriptors for **4a–h** (for a full set of substrates, see the Supporting Information) were calculated from the TS of the corresponding thionium cation in the uncatalyzed cyclization.[22] Comparison of the enantioselectivity and the corresponding parameters resulted in the statistical model in Figure 1b ($R^2 = 0.86$, intercept $= 0.13$, L1O $= 0.81$), which contains two parameters condensed into one term. The simple equation obtained can be readily interpreted. $B5_{Ar}$ accounts for either the steric hindrance or the shape of the aryl substituent, and NBO_{AlkH} describes the average charge of the thionium alkyl chain. The presence of this latter descriptor in the model supports the importance of the interaction highlighted in **TS-R**. Moreover, calculation of the electron density map of the uncatalyzed TS for the benchmark substrate **6d**, showed that the acidic N−H proton and the alkyl chain close to the thionium cation were the most electron-poor regions of the cyclizing substrate (Figure 1d). Thus, the TS computational analysis and the multidimensional correlation analyses agree as a mutual validation of the presented results.

In summary, we have developed an oxidative Pummerer-type cyclization for the synthesis of cyclic *N,S*-acetals from readily available starting materials. This operationally simple and mild protocol provides a powerful means to access a broad range of enantioenriched cyclic *N,S*-acetals using an anionic phase-transfer catalyst. Deuterium-labelling experiments were performed to identify the stereodiscrimination step of this process. Additionally, the origin of the enantioselectivity was investigated by DFT TS analysis and by multidimensional correlation techniques, which revealed that a set of subtle yet important NCIs are responsible for the observed level of enantioselectivity (up to 92% *ee*).

Conflict of interest

The authors declare no conflict of interest.

[1] a) R. Pummerer, *Ber. Dtsch. Chem. Ges.* **1909**, *42*, 228–232; b) R. Pummerer, *Ber. Dtsch. Chem. Ges.* **1910**, *43*, 1401–1412.

[2] Reviews about transformations based on Pummerer reactions: a) S. K. Bur, A. Padwa, *Chem. Rev.* **2004**, *104*, 2401–2432; b) K. S. Feldman, *Tetrahedron* **2006**, *62*, 5003–5034; c) L. H. S. Smith, S. C. Coote, H. F. Sneddon, D. J. Procter, *Angew. Chem. Int. Ed.* **2010**, *49*, 5832–5844; *Angew. Chem.* **2010**, *122*, 5968–5980; d) A. P. Pulis, D. J. Procter, *Angew. Chem. Int. Ed.* **2016**, *55*, 9842–9860; *Angew. Chem.* **2016**, *128*, 9996–10014; e) A. Shafir, *Tetrahedron Lett.* **2016**, *57*, 2673–2682.

[3] For examples of asymmetric Pummerer reactions using enantio-pure sulfoxides, see: a) K. S. Feldman, A. G. Karatjas, *Org. Lett.* **2004**, *6*, 2849–2852; b) J. L. García Ruano, J. Alemn, M. T. Aranda, M. J. Aryalo, A. Padwa, *Org. Lett.* **2005**, *7*, 19–22; c) Y. Nagao, S. Miyamoto, M. Miyamoto, H. Takeshige, K. Hayashi, S. Sano, M. Shiro, K. Yamaguchi, Y. Sei, *J. Am. Chem. Soc.* **2006**, *128*, 9722–9729.

[4] For reviews on transition-metal-catalyzed C−S bond-forming reactions, see: a) T. Kondo, T.-A. Mitsudo, *Chem. Rev.* **2000**, *100*, 3205–3220; b) T. W. Lyons, M. S. Sanford, *Chem. Rev.* **2010**, *110*, 1147–1169; c) I. P. Beletskaya, V. P. Ananikov, *Chem. Rev.* **2011**, *111*, 1596–1636; For organocatalytic C−S bond formations, see: d) P. Chauhan, S. Mahajan, D. Enders, *Chem. Rev.* **2014**, *114*, 8807–8864; For leading books, see: e) *Organosulfur Chemistry in Asymmetric Synthesis* (Eds.: T. Toru, C. Bolm), Wiley-VCH, Weinheim, **2008**; f) P. Bichler, J. A. Love, *Top. Organomet. Chem.* **2010**, *31*, 39–64.

[5] a) C. Chatgilialoglu, K. D. Asmus, *Sulfur-Centered Reactive Intermediates in Chemistry and Biology*, Springer, New York, **1991**; b) J. J. R. Fraústo da Silva, R. J. P. Williams, *The Biological Chemistry of the Elements*, Clarendon Press, Oxford, **2001**; c) K. Yamamoto, K. Fujita, K. Tabashi, Y. Kawashima, E. Kato, M. Oya, J. Iwao, *J. Med. Chem.* **1988**, *31*, 919–930; d) N. T. Burford, M. J. Clark, T. S. Wehrman, S. W. Gerritz, M. Banks, J. O'Connell, J. R. Traynor, A. Alt, *Proc. Natl. Acad. Sci. USA* **2013**, *110*, 10830–10835.

[6] V. Rauniyar, A. D. Lackner, G. L. Hamilton, F. D. Toste, *Science* **2011**, *334*, 1681–1684.

[7] a) A. J. Neel, J. P. Hehn, P. F. Tripet, F. D. Toste, *J. Am. Chem. Soc.* **2013**, *135*, 14044–14047; b) A. J. Neel, A. Milo, F. D. Toste, M. S. Sigman, *Science* **2015**, *347*, 737–743.

[8] For examples of oxidative Pummerer reactions, see: a) R. A. McCormick, K. M. James, N. Willetts, D. J. Procter, *QSAR Comb. Sci.* **2006**, *25*, 709–712; b) Z. Li, H. Li, X. Guo, L. Cao, R. Yu, H. Li, S. Pan, *Org. Lett.* **2008**, *10*, 803–805.

[9] For examples of enantioselective synthesis of acyclic *N,S*-acetals, see: a) S. Nakamura, S. Takahashi, D. Nakane, H. Masuda, *Org. Lett.* **2015**, *17*, 106–109; b) C. Baceño, P. Chauhan, A. Rembiak, A. Wang, D. Enders, *Adv. Synth. Catal.* **2015**, *357*, 672–676; c) J. Suć, I. Dokli, M. Gredičak, *Chem. Commun.* **2016**, *52*, 2071–2074; d) G. K. Ingle, M. G. Mormino, L. Wojtas, J. C. Antilla, *Org. Lett.* **2011**, *13*, 4822–4825; e) X. Fang, Q.-H. Li, H.-Y. Tao, C.-J. Wang, *Adv. Synth. Catal.* **2013**, *355*, 327–331; f) H.-Y. Wang, J.-X. Zhang, D.-D. Cao, G. Zhao, *ACS Catal.* **2013**, *3*, 2218–2221; g) H. Qian, J. Sun, *Asian J. Org. Chem.* **2014**, *3*, 387–390; For phosphoric acid catalyzed enantioselective *N,O*-, *O,O*-, *N,N*-, *S,S*-acetal synthesis, see: h) G. Li, F. R. Fronczek, J. C. Antilla, *J. Am. Chem. Soc.* **2008**, *130*, 12216–12217; i) Z. Sun, G. A. Winschel, A. Borovika, P. Nagorny, *J. Am. Chem. Soc.* **2012**, *134*, 8074–8077; j) I. Čorić, S. Vellalath, B. List, *J. Am. Chem. Soc.* **2010**, *132*, 8536–8537; k) G. B. Rowland, H. Zhang, E. B. Rowland, S. Chennamadhavuni, Y. Wang, J. C. Antilla, *J.*

Am. Chem. Soc. **2005**, *127*, 15696–15697; l) X. Cheng, S. Vellalth, R. Goddard, B. List, *J. Am. Chem. Soc.* **2008**, *130*, 15786–15787; m) M. Rueping, A. P. Antonchick, E. Sugiono, K. Grenader, *Angew. Chem. Int. Ed.* **2009**, *48*, 908–910; *Angew. Chem.* **2009**, *121*, 925–927; n) A. Alix, C. Lalli, P. Retailleau, G. Masson, *J. Am. Chem. Soc.* **2012**, *134*, 10389–10392; o) J.-S. Yu, W.-B. Wu, F. Zhou, *Org. Biomol. Chem.* **2016**, *14*, 2205–2209.

[10] J. M. Bobbit, C. Brücker, N. Merbouh, *Org. React.* **2010**, *74*, 103–424.

[11] For a recent review of oxoammonium salts used in dehydrogenative coupling reactions, see: a) O. García Mancheño, T. Stopka, *Synthesis* **2013**, *45*, 1602–1611; For recent examples: b) H. Richter, O. Mancheño, *Eur. J. Org. Chem.* **2010**, 4460–4467; c) H. Richter, O. García Mancheño, *Org. Lett.* **2011**, *13*, 6066–6069; d) S. Wertz, S. Kodama, A. Studer, *Angew. Chem. Int. Ed.* **2011**, *50*, 11511–11515; *Angew. Chem.* **2011**, *123*, 11713–11717.

[12] For selected examples of the oxidation of alcohols using oxoammonium salts, see: a) J. M. Bobbitt, *J. Org. Chem.* **1998**, *63*, 9367–9374; b) A. De Mico, R. Margarita, L. Parianti, A. Vescovi, G. Piancatelli, *J. Org. Chem.* **1997**, *62*, 6974–6977; c) J. Einhorn, C. Einhorn, F. Ratajczak, J.-L. Pierre, *J. Org. Chem.* **1996**, *61*, 7452–7454.

[13] Full data of the optimization study is given in the Supporting Information.

[14] This might be because of the low stability of 2,2,6,6-tetramethylpiperidine-1-oxoammonium tetrafluroborate salt in solvent. See Ref. [12a] for more details.

[15] M. S. Sigman, K. C. Harper, E. N. Bess, A. Milo, *Acc. Chem. Res.* **2016**, *49*, 1292–1301.

[16] a) E. Yamamoto, M. J. Hilton, M. Orlandi, V. Saini, F. D. Toste, M. S. Sigman, *J. Am. Chem. Soc.* **2016**, *138*, 15877–15880; b) M. Orlandi, J. A. S. Coelho, M. J. Hilton, F. D. Toste, M. S. Sigman, *J. Am. Chem. Soc.* **2017**, *139*, 6803–6806; c) M. Orlandi, M. J. Hilton, E. Yamamoto, F. D. Toste, M. S. Sigman, *J. Am. Chem. Soc.* **2017**, *139*, 12688–12695.

[17] A. Milo, E. N. Bess, M. S. Sigman, *Nature* **2014**, *507*, 210–214.

[18] K. C. Harper, E. N. Bess, M. S. Sigman, *Nat. Chem.* **2012**, *4*, 366.

[19] a) R. R. Knowles, E. N. Jacobsen, *Proc. Natl. Acad. Sci. USA* **2010**, *107*, 20678–20685; b) E. H. Krenske, K. N. Houk, *Acc. Chem. Res.* **2013**, *46*, 979–989; c) J. P. Wagner, P. R. Schreiner, *Angew. Chem. Int. Ed.* **2015**, *54*, 12274–12296; *Angew. Chem.* **2015**, *127*, 12446–12471; d) S. E. Wheeler, T. J. Seguin, Y. Guan, A. C. Doney, *Acc. Chem. Res.* **2016**, *49*, 1061–1069; e) F. Duarte, R. S. Paton, *J. Am. Chem. Soc.* **2017**, *139*, 8886–8896.

[20] a) A. J. Neel, M. J. Hilton, M. S. Sigman, F. D. Toste, *Nature* **2017**, *543*, 637–646; b) B. Bhaskararao, R. B. Sunoj, *J. Am. Chem. Soc.* **2015**, *137*, 15712–15722; c) T. J. Seguin, S. E. Wheeler, *ACS Catal.* **2016**, *6*, 7222–7228; d) T. J. Seguin, S. E. Wheeler, *Angew. Chem. Int. Ed.* **2016**, *55*, 15889–15893; *Angew. Chem.* **2016**, *128*, 16121–16125; e) T. J. Seguin, S. E. Wheeler, *ACS Catal.* **2016**, *6*, 2681–2688; See also [17b] and [20e].

[21] a) J. Greindl, J. Hioe, N. Sorgenfrei, F. Morana, R. M. Gschwind, *J. Am. Chem. Soc.* **2016**, *138*, 15965–15971; b) N. Sorgenfrei, J. Hioe, J. Greindl, K. Rothermel, F. Morana, N. Lokesh, R. M. Gschwind, *J. Am. Chem. Soc.* **2016**, *138*, 16345–16354.

[22] M. Orlandi, F. D. Toste, M. S. Sigman, *Angew. Chem. Int. Ed.* **2017**, *56*, 14080–14084; *Angew. Chem.* **2017**, *129*, 14268–14272.